

Ab initio recombination in the expanding ultracold plasmas

Yuri V. Dumin^{1, 2, a)} and Ludmila M. Svirskaya^{3, 4, b)}

¹⁾*Lomonosov Moscow State University, Sternberg Astronomical Institute, Universitetskii prosp. 13, 119234 Moscow, Russia*

²⁾*Space Research Institute of Russian Academy of Sciences, Profsoyuznaya str. 84/32, 117997 Moscow, Russia*

³⁾*South Ural State University, Prosp. Lenina 76, 454080 Chelyabinsk, Russia*

⁴⁾*South Ural State Humanitarian Pedagogical University, Prosp. Lenina 69, 454080 Chelyabinsk, Russia*

(Dated: 28 December 2025)

The efficiency of recombination is of crucial importance for the existence of ultracold plasmas, particularly, the ones formed in the magneto-optical traps. Unfortunately, a straightforward simulation of the recombination encounters the problem of huge difference in the spatial and temporal scales for free and bound motion of the electrons. As a result, only the “virtual” electron-ion pairs are usually reproduced in such simulations, and it is necessary to employ some additional criteria to identify them with the recombined atoms (this might be a minimal number of revolutions of the electron about the nearest ion or a maximal distance between them). It is the aim of this paper to present the first successful *ab initio* simulation of the recombination without any auxiliary assumptions. We employed a special algorithm, which was based on: (i) using the “scalable” reference frame, co-moving with the expanding plasma, (ii) dynamical choice of the number of “mirror” cells, taking into account in calculation of the Coulomb sums, and (iii) accurate treatment of the singular interparticle interactions, without any truncation or “softening” of the Coulomb forces. Then, the recombination events are identified by a series of sharp equidistant peaks in the kinetic and/or potential energies for a sample of particles, which are caused by the captured electrons passing near the pericenters of their orbits; and this is confirmed by a detailed inspection of the particle trajectories. Thereby, we were able to trace formation of the real—rather than “virtual”—electron-ion pairs. The total efficiency of recombination for the realistic experimental conditions was found to be about 20%, which is in perfect agreement both with the laboratory measurements and with the earlier semi-empirical simulations.

I. INTRODUCTION

The ultracold plasmas (UCP), formed after release of the bunches of photoionized atoms from the magneto-optical traps¹, represent a relatively new branch of plasma physics, emerged in the very late 1990s and early 2000s^{2–5}. The possibility of existence of such plasmas for an appreciable time intervals crucially depends on the efficiency of recombination, since it might be intuitively expected that the charged particles with a sufficiently strong Coulomb coupling will quickly collapse into the neutral pairs.

It is interesting to mention that the corresponding numerical simulations started already in the early 1990’s, *i.e.*, a decade before the first experiments with UCP. Surprisingly, these simulations demonstrated that the ultracold plasmas experienced a very small recombination, *i.e.*, could survive for a sufficiently long time⁶. Unfortunately, it was suspected by some opponents that the anomalous resistance of charged particles with respect to the recombination might be just an artifact of the particular numerical methods. For example, the recombined neutral pairs could be efficiently destroyed by the collisions with walls of the computational box^{7,8}, if the reflective boundary conditions are imposed there. Moreover, the anomalously small recombination rate might be caused just by the accumulation of numerical errors, preventing formation of the

bound electron-ion pairs. This problem is especially severe because of the huge difference in the characteristic temporal and spatial scales for the free and bound motion of the charged particles in plasmas.

In view of the above-mentioned problems, the most of works on recombination in UCP employed a semi-empirical two-step procedure: Firstly, the electron distribution function was simulated numerically by the molecular-dynamic approach, and then it was used for analytical estimates of the recombination rate, *e.g.*, employing the idea of electron diffusion in the energetic space⁹.

On the other hand, as regards the *ab initio* modeling of recombination, the most of works employed some artificial criteria for the formation of bound electron-ion pairs: For example, it was assumed that the act of recombination took place if an electron performed a certain number of revolutions about the nearest ion (*e.g.*, 4 complete revolutions)¹⁰. Yet another approach was to assume that all electrons located closer than a specified distance from the nearest ions (*e.g.*, 20% of the Wigner–Seitz radius) will ultimately recombine¹¹. Such artificial criteria were necessary because the commonly-used numerical schemes did not allow ones to get the sufficiently stable electron-ion pairs: they were destroyed rather quickly due to accumulation of the computational errors.

It is the aim of the present work to describe a specially designed numerical algorithm that is really able to trace formation of the stable electron-ion pairs and, therefore, to serve as a testbed for other methods. In fact, this algorithm closely resembles the one employed in our earlier paper¹², which was aimed at *ab initio* simulation of the electron temperature evo-

^{a)}Electronic mail: dumin@pks.mpg.de, dumin@yahoo.com

^{b)}Electronic mail: svirskajalm@susu.ru, svirskajalm@mail.ru

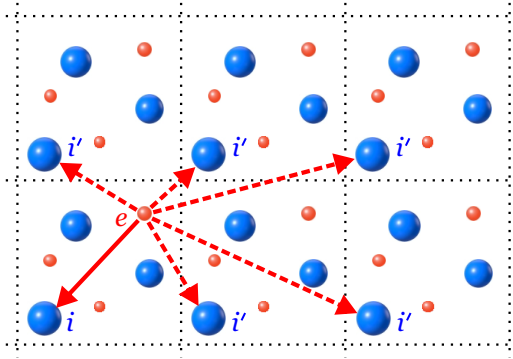


FIG. 1. Sketch of calculation of the Coulomb sums, where each electron e interacts not only with a specified ion i in the basic cell (solid arrow) but also with infinite number of its mirror images i' (dashed arrows).

lution in ultracold plasma bunches experiencing a considerable expansion. The simulated dependence $T_e \propto t^\alpha$ with exponent $\alpha \in [-1.25, -1.08]$ turned out to be in perfect agreement with the results of experiment¹³, where $\alpha = -(1.2 \pm 0.1)$. It is important to emphasize that this coincidence was achieved exactly from “the first principles”, without postulation of any additional heat sources or sinks. As will be seen below, the same numerical scheme provides also very good results in the simulation of recombination.

II. THE ALGORITHM OF SIMULATION

A. Geometrical configuration

We shall consider an infinite volume of plasma expanding uniformly in all directions. It is assumed to be composed of the identical cubic cells filled with some number of ions and the same number of electrons, as illustrated in Fig. 1. Then, the Coulomb forces are calculated between all particles in this system *i.e.*, not only within the same basic cell but also with all its “mirror” images:

$$\begin{aligned} \mathbf{F}_i = & \sum_{j=1}^N e^2 \frac{\mathbf{R}_j - \mathbf{r}_i}{|\mathbf{R}_j - \mathbf{r}_i|^3} + \sum_{j=1, j \neq i}^N e^2 \frac{\mathbf{r}_i - \mathbf{r}_j}{|\mathbf{r}_i - \mathbf{r}_j|^3} \\ & + \sum_{k=1}^3 \sum_{n_k=-\infty, n_k \neq 0}^{+\infty} \left\{ \sum_{j=1}^N e^2 \frac{[\mathbf{R}_j + L \sum_{l=1}^3 n_l \mathbf{e}_l] - \mathbf{r}_i}{|[\mathbf{R}_j + L \sum_{l=1}^3 n_l \mathbf{e}_l] - \mathbf{r}_i|^3} \right. \\ & \left. + \sum_{j=1}^N e^2 \frac{\mathbf{r}_i - [\mathbf{r}_j + L \sum_{l=1}^3 n_l \mathbf{e}_l]}{|\mathbf{r}_i - [\mathbf{r}_j + L \sum_{l=1}^3 n_l \mathbf{e}_l]|^3} \right\}. \end{aligned} \quad (1)$$

Here, \mathbf{F}_i is the force acting on the i 'th electron, \mathbf{r}_j and \mathbf{R}_j ($j = 1, \dots, N$) are the electronic and ionic coordinates, N is the number of charged particles of each kind in the basic cell, e is the electron charge, L is the linear size of the basic cell, \mathbf{e}_l ($l = 1, 2, 3$) are the unitary vectors of the Cartesian coordinate system, and subscripts n_k ($k = 1, 2, 3$) specify the number of the mirror cell in each direction. We do not write here a similar formula for the forces acting on ions: since the ions

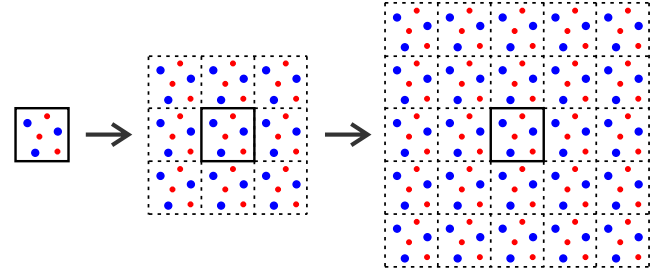


FIG. 2. Sketch of summation over the mirror cells (dotted squares) around the basic cell (solid square) in calculation of the Coulomb forces.

are much more massive than electrons, they can be usually assumed to move by inertia (some additional explanations will be given below).

In fact, summation in formula (1) is performed over a finite number of mirror cells until the specified accuracy of convergence of the Coulomb forces is achieved. These mirror cells are arranged into the cubic shells of increasing radii around the basic cell; see Fig. 2. Therefore, although we used a relatively small number of charged particles in the basic cell (*e.g.* a few dozens or a few hundreds), the total number of particles taken into account in calculation of the Coulomb sums becomes huge. For example, if the relative accuracy of calculation is specified to be about 10^{-5} , then even at $N = 10$ the total number of particles involved in the computation turns out to be from a few hundred thousand to a few million. Let us emphasize that this number is not fixed but chosen dynamically at each step of integration.

Of course, a possible alternative to the straightforward summation over the cells, might be the well-known Ewald procedure, whose original idea can be found, *e.g.*, in monograph¹⁴ and more elaborated versions in paper¹⁵. However, since our original intention was to follow the *ab initio* approach as strictly as possible, we did not use here the Ewald approximation.

B. The scalable reference frame

Yet another serious problem in simulation of the expanding plasma clouds is a considerable change in the spatial scale of the system—and, therefore, in the Coulomb forces—in the course of time, which makes it difficult to keep the accuracy of integration at a stable level. To get around this obstacle, we introduce the scalable reference frame, expanding with the average expansion rate of the plasma. Namely, a length of the basic cell is assumed to increase as

$$L(t) = L_0 + u_0 t, \quad (2)$$

where L_0 is its initial value, and u_0 is the velocity of expansion. From the physical point of view, such a linear law corresponds to the inertial stage of the plasma motion, when the most part of its initial thermal energy was transformed into kinetic energy of the macroscopic expansion. In fact, this law

is established very quickly, and it is commonly used in the interpretation of all experiments with UCP.

Besides, it is convenient to introduce the following dimensionless variables. Let the unit of length be the time-dependent characteristic interparticle separation:

$$\tilde{l}(t) = L(t)/(2N)^{1/3}. \quad (3)$$

The unit of time is taken to be proportional to the characteristic period of oscillations of an electron with mass m_e in the field of the nearest ion at the initial instant of time:

$$\tau = (m_e^{1/2}/e) \tilde{l}_0^{3/2} \quad (4)$$

(as distinct from the unit of length, it is independent of time). From here on, all physical quantities normalized to \tilde{l} and τ will be marked by asterisks.

As can be easily seen, the unit of length varies with the dimensionless time as

$$\tilde{l} = \tilde{l}_0 (1 + u_0^* t^*), \quad (5)$$

where

$$u_0^* = u_0 \tau / L_0 \quad (6)$$

is the dimensionless velocity of expansion; while the dimensionless size of the basic cell remains constant:

$$L^* = (2N)^{1/3}. \quad (7)$$

In other words, the simulated particles perform their motion in a box of the fixed size (7), thereby mitigating the problem of very large variation of the spatial coordinates in the case of considerable plasma expansion. As usual, the periodic boundary conditions are imposed at the box boundaries: when one of the particles leaves the box through one of its faces, the identical particle with the same velocity enters the box through the opposite face.

The classical equation of motion of the i 'th electron,

$$m_e d^2 \mathbf{r}_i / dt^2 = \mathbf{F}_i, \quad (8)$$

in the scale-dependent dimensionless variables (4) and (5) is reduced to

$$\ddot{\mathbf{r}}_i^* + 2u_0^*(1 + u_0^* t^*)^{-1} \dot{\mathbf{r}}_i^* = (1 + u_0^* t^*)^{-3} \mathbf{F}_i^*, \quad (9)$$

where dot denotes a derivative with respect to t^* . Therefore, expansion of the coordinate frame results in the appearance of an effective viscous force, proportional to the electron velocity, which is presented by the second term in the left-hand side of this equation. In fact, just this dissipative force is responsible for the electron deceleration and its subsequent trapping by the nearest ion.

The Coulomb forces, originally given by formula (1), after the normalization are reduced to

$$\begin{aligned} \mathbf{F}_i^* = & \sum_{j=1}^N \frac{\mathbf{R}_j^* - \mathbf{r}_i^*}{|\mathbf{R}_j^* - \mathbf{r}_i^*|^3} + \sum_{j=1, j \neq i}^N \frac{\mathbf{r}_i^* - \mathbf{r}_j^*}{|\mathbf{r}_i^* - \mathbf{r}_j^*|^3} \\ & + \sum_{k=1}^3 \sum_{n_k=-\infty, n_k \neq 0}^{+\infty} \left\{ \sum_{j=1}^N \frac{[\mathbf{R}_j^* + L^* \sum_{l=1}^3 n_l \mathbf{e}_l] - \mathbf{r}_i^*}{|[\mathbf{R}_j^* + L^* \sum_{l=1}^3 n_l \mathbf{e}_l] - \mathbf{r}_i^*|^3} \right. \\ & \left. + \sum_{j=1}^N \frac{\mathbf{r}_i^* - [\mathbf{r}_j^* + L^* \sum_{l=1}^3 n_l \mathbf{e}_l]}{|\mathbf{r}_i^* - [\mathbf{r}_j^* + L^* \sum_{l=1}^3 n_l \mathbf{e}_l]|^3} \right\}. \end{aligned} \quad (10)$$

As was already explained above, the sums over k and n_k are actually calculated over the cubic shells of increasing radii, composed of the “mirror” cells, until the required accuracy of convergence is achieved.

C. The method of integration

Following the standard procedure, the second-order differential equation (9) can be rewritten as a system of two first-order differential equations:

$$\dot{\mathbf{r}}_i^* = \mathbf{v}_i^*, \quad (11a)$$

$$\dot{\mathbf{v}}_i^* = -2u_0^* s \mathbf{v}_i^* + s^3 \mathbf{F}_i^*, \quad (11b)$$

where

$$s(t^*) = (1 + u_0^* t^*)^{-1}. \quad (12)$$

Next, they are integrated numerically by the second-order Runge–Kutta method with a constant stepsize. In fact, this method is rather inefficient, and a much better computational performance could be achieved by using the higher-order integrators with adaptive stepsize control. This was done, for example, in our earlier works^{16,17}, where we employed subroutines from the *Numerical Recipes* library¹⁸. Unfortunately, the adaptive stepsize control operates reliably only for the reflective boundaries and encounters serious problems in the case of periodic boundary conditions (for more details, see Appendix A in paper¹⁶). So, since the geometrical setup of our simulations (Fig. 1) inherently incorporates the periodic boundaries, we had to use a rather primitive integration scheme.

Yet another very subtle point of our modeling is usage of the exact (singular) Coulomb potentials of the charged particles, without any softening or cut-offs at the small distances, which was a common practice in many earlier papers^{11,19,20}. We preferred to avoid such a simplification, because formation of the bound states (resulting in the recombination) is rather sensitive to the specific form of the potential. Particularly, the closed trajectories are possible only in the exact Coulomb field²¹. (Yet another option for the formation of closed orbits might be the potential of harmonic oscillator, proportional to r^2 ; but this is beyond our physical context.)

Unfortunately, if the simulated plasma was initially cold enough, then the electrons begin to fall onto the nearest ions, sometimes resulting in the almost head-on collisions, which cannot be resolved by our integration algorithm. (Such cases can be identified by the sharp jumps in total kinetic energy of the electrons and/or asymmetric profiles of the kinetic energy with respect to a pericenter of the electron orbit.) Then, the integration was canceled, and the corresponding initial conditions were discarded. So, we employed only the “favorable” initial conditions, which do not lead to failures in the very beginning of simulations. In fact, the number of failures was an order of magnitude greater than the number of favorable cases. However, this did not increase dramatically the computational cost of our simulations, because the failures typically occurred at the very early stage of the integration (about a few τ from

the beginning), while we were interested in the long-term dynamics (a few hundred or thousand τ). So, a dozen of failures did not take too much time.

D. Initial conditions

An accurate specification of the initial conditions for ultracold plasmas is a rather nontrivial task. For example, if the plasma is produced by *instantaneous* photoionization of neutral atoms, the initial electron positions should be substantially correlated with the ionic ones, and the distribution of their velocities will be non-Gaussian¹¹. In the opposite case, when the ionization process takes some time, the released electrons will be mixed in space between the ions and approximately thermalized, resulting in the uniform coordinate and Gaussian velocity distributions. Since we are interested in the recombination events occurring after a sufficiently long temporal evolution, exact specification of the initial conditions should not be important. So, for the sake of simplicity, we shall follow the second option. Namely, initial positions of the electrons r_{i0}^* and ions R_{i0}^* ($i = 1, \dots, N$) will be given by random numbers distributed uniformly within the box, $-L^*/2 \leq (x^*, y^*, z^*) \leq L^*/2$.

On the other hand, the initial electron velocities \dot{r}_{i0}^* will be specified by the normal (Gaussian) distribution with a root-mean-square deviation σ_{v0}^* over each Cartesian coordinate. This quantity evidently characterizes the initial electron temperature. As was shown in our work¹², the formal definition $T_e = (2/3)K_e/k_B$ (where K_e is the electron kinetic energy, and k_B is the Boltzmann constant) should work rather well even for the electrons strongly interacting with ions. At last, as was already mentioned above, the ions are assumed to move by inertia due to their very large masses, *i.e.*, in the co-moving reference frame, $R_i^* = \text{const}$ and $\dot{R}_i^* = 0$.

III. RESULTS OF THE SIMULATIONS

The simulations were performed for various numbers of the charged particles of each kind N in the basic cell, from 10 to 1000. Since the employed algorithm of numerical integration—without the adaptive stepsize control—was computationally expensive, a sufficiently long interval of integration (about 1000τ) was achieved only at the small number of particles (*e.g.*, $N = 10$); and the most convincing patterns of recombination were obtained just in this case. On the other hand, when N was substantially larger, the achievable interval of integration was a few times shorter; so that only the initial stage of recombination was observed. (To avoid misunderstanding, let us remind once again that the actual number of particles taken into account in calculation of the Coulomb forces, including the “mirror” cells, was much greater: for example, even at $N = 10$ it varied from a few hundred thousand to a few million, depending on the rate of convergence of the Coulomb sums at each particular step of integration.) In the results presented below, we used the initial dispersion of the electron velocities $\sigma_{v0}^* = 3.0$. In other words, the plasma was

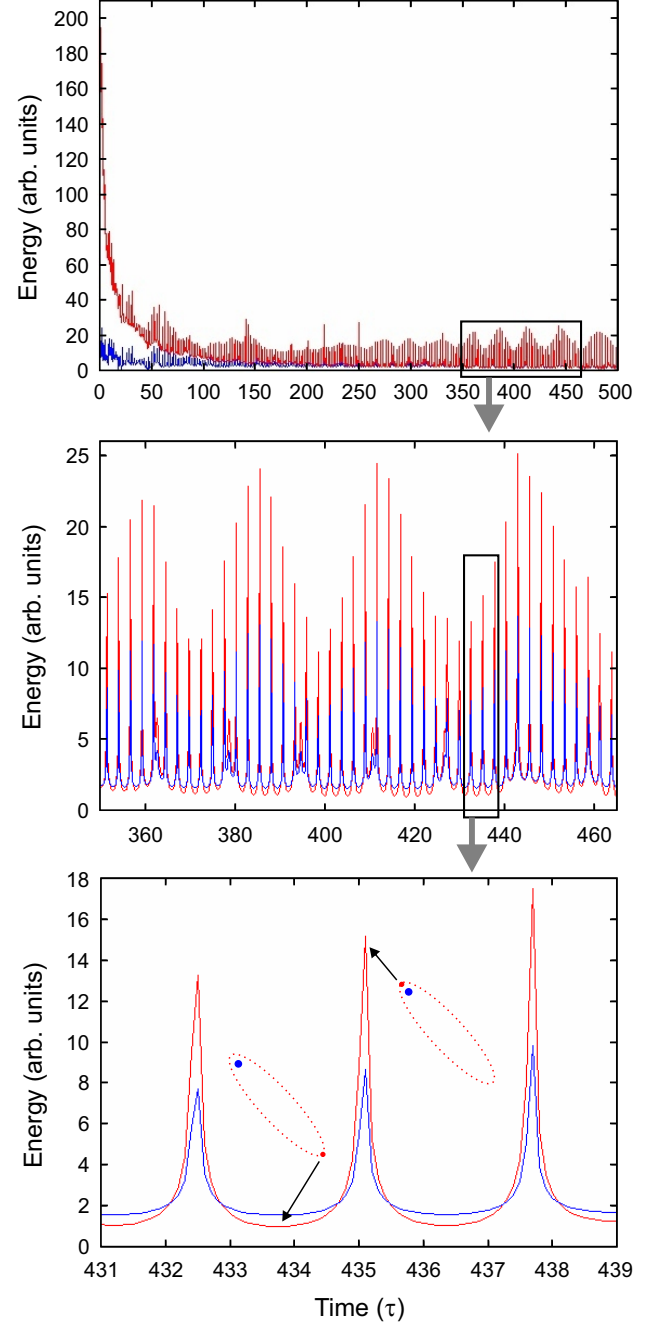


FIG. 3. Temporal dependence of the kinetic (red curves) and potential (blue curves) energies of all particles in the basic cell at various “magnifications” (successive panels, from top to bottom). The regions of subsequent magnification are marked by the rectangles.

originally weakly non-ideal, since its initial kinetic energy exceeded the potential one by an order of magnitude. The overall plasma expansion rate was taken to be $u_0^* = 0.1$.

Figure 3 shows a temporal behavior of the total kinetic and potential energies of all particles in the basic cell, including the energy of interaction with the “mirror” images. As can be expected, in the upper panel one can see initially a sharp decay in the kinetic energy, which is just an adiabatic cool-

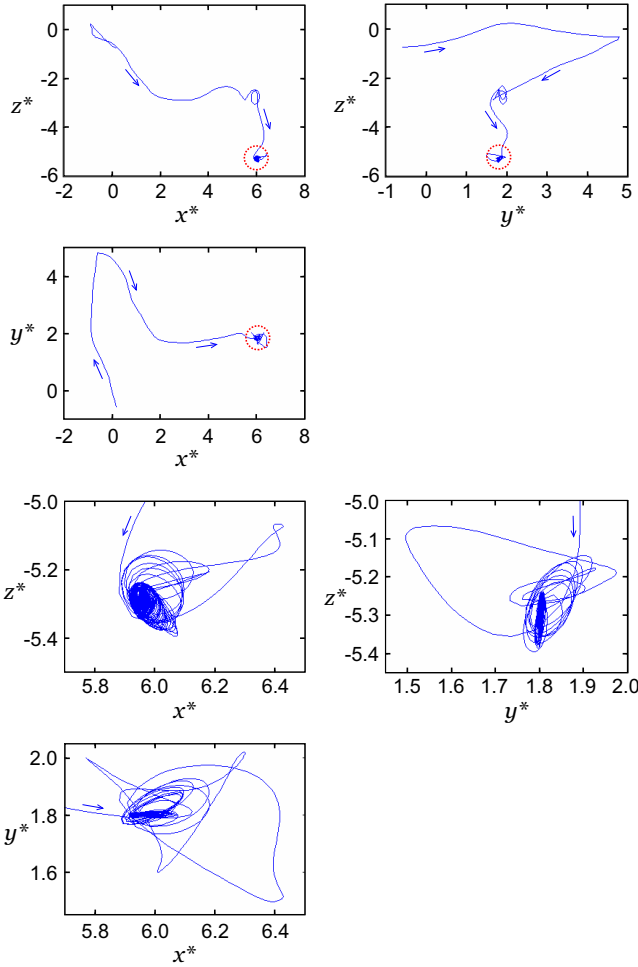


FIG. 4. Trajectory of the first (short-period) captured electron viewed in three coordinate planes at two different magnifications (three top and three bottom panels, respectively). The region of formation of a captured state of the electron is marked by the red dotted circle. The coordinate scales in various directions are different.

ing of the expanding plasma. A much more interesting and nontrivial feature is that this cooling is associated with a development of fast oscillations (a series of the sharp equidistant peaks), surviving up to the end of simulation (which was about two times longer than the time interval presented in figure). Moreover, starting from $250-300 \tau$ one can see onset of the second, much larger period of modulation, which also survives up to the end of our simulation. The presence of these two periods is clearly seen in the second, enlarged panel. At last, inspection of the third, most magnified panel gives us a hint that the modulation of the kinetic and potential energies is caused just by the passages of an electron, captured into a strongly elliptical orbit, near the pericenter and apocenter of its trajectory.

A more careful analysis of the electron trajectories, presented in Figs. 4 and 5, confirms this conjecture. It is seen that the above-mentioned electrons—after some periods of a “random walk”—really form the confined states in the co-moving reference frame. So, they should result in the recombination

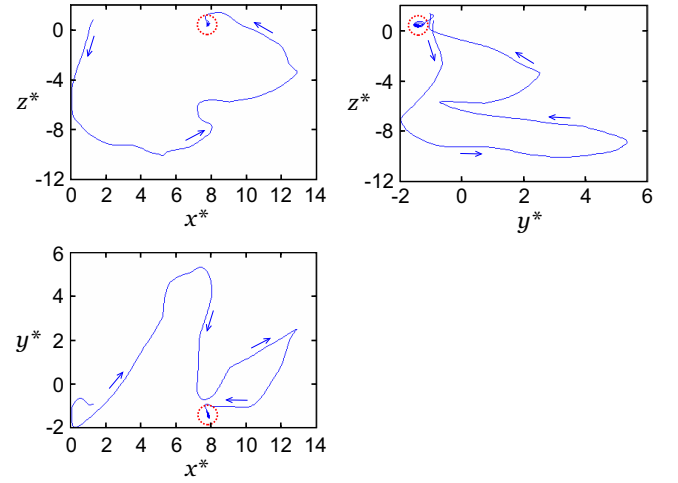


FIG. 5. Trajectory of the second (long-period) captured electron viewed in three coordinate planes. The region of formation of a captured state of the electron is marked by the red dotted circle. The coordinate scales in various directions are different.

with the corresponding ions if quantum effects will be taken into account.

The trajectories of other eight electrons in the basic cell do not exhibit any features of localization. Consequently, we can estimate the total efficiency of recombination as 20%. This is actually the main result of our simulations.

IV. DISCUSSION

Although the employed sample of particles was very small (10 electrons and 10 ions in the basic cell), the results obtained are in agreement with the experimental measurements²² as well as with the earlier modeling¹¹. In the last-cited paper, the criterion of recombination was introduced rather formally as the percentage of electrons located closer than the specified distance (e.g., 0.2 Wigner–Seitz radius) to the nearest ion. Surprisingly, this semi-empirical criterion gave approximately the same result, 17–18 %, as our *ab initio* approach.

Yet another widely-used criterion¹⁰ is to find the electrons that performed a specified minimal number of revolutions (e.g., 1, 2, 4, or 6) about the nearest ion and to assume that they will ultimately recombine to the neutral atoms. In fact, this approach is even more popular and often considered as justified better. Unfortunately, analysis of the results of our simulations did not provide any significant support in favor of this criterion. So, this subject still needs to be studied in more detail.

As was already mentioned above, the number of particles in the basic cell simulated in detail by our method, $N = 10$, was rather small. This was because each computational run on the ordinary PC, without a parallelization, took a few months. So, when the number of particles was much greater, e.g. 100 or 1000, we were able to perform the simulation only at the considerably shorter time intervals, about 100τ , when the recombination process was not yet complete.

The low speed of calculations was caused by the fact that we employed neither the adaptive stepsize control for integration, nor Ewald summation technique for the Coulomb sums. Unfortunately, when these methods were used in our earlier attempts, we were unable to reproduce the captured electron trajectories at all, most probably, because of the additional errors introduced by the corresponding procedures. So, we used here a more straightforward approach. However, one can expect that it will be possible in future to introduce the adaptive stepsize control and Ewald summation into our algorithm of the scalable (co-moving) reference frame, which should make this approach much more efficient computationally.

V. CONCLUSIONS

1. To the best of our knowledge, the performed work is the first successful attempt of *ab initio* simulation of recombination in the expanding ultracold plasmas, which clearly demonstrates how some of electrons become localized and form the stable compact pairs with the respective ions.
2. A cornerstone of our approach is employing the scalable reference frame, co-moving with the expanding plasma. Such transformation formally converts the effect of overall plasma expansion into the effective frictional force in the fixed coordinate frame. This enables us both to avoid some computational problems and to simplify interpretation of the results of simulation.
3. The efficiency of recombination obtained by this method (about 20% for the realistic experimental conditions) turns out to be in agreement both with the values derived by some semi-empirical approaches¹¹ and with the laboratory measurements²².
4. Unfortunately, the proposed modeling scheme is rather expensive computationally. Therefore, it is primarily intended for testing the accuracy of other (semi-empirical) methods rather than for a routine usage. However, it is expected that the efficiency of this approach can be increased in future by introducing new versions of the adaptive stepsize control for the numerical integration and the refined Ewald summation procedures for calculation of the Coulomb sums.

ACKNOWLEDGMENTS

YVD is grateful to A.A. Bobrov, P.R. Levashov, S.A. Mayorov, J.-M. Rost, S.A. Saakyan, U. Saalmann, V.S. Vorob'ev, B.B. Zelener, and B.V. Zelener for fruitful discussions and valuable suggestions.

AUTHOR DECLARATIONS

Conflict of Interest

The authors have no conflicts to disclose.

DATA AVAILABILITY

The data that support the findings of this study are available from the corresponding author upon reasonable request.

References:

- ¹T. Killian, S. Kulin, S. Bergeson, L. Orozco, C. Orzel, and S. Rolston, “Creation of an ultracold neutral plasma,” *Phys. Rev. Lett.* **83**, 4776 (1999).
- ²P. Gould and E. Eyler, “Ultracold plasmas come of age,” *Phys. World* **14**(3), 19 (2001).
- ³S. Bergeson and T. Killian, “Ultracold plasmas and Rydberg gases,” *Phys. World* **16**(2), 37 (2003).
- ⁴T. Killian, “Ultracold neutral plasmas,” *Science* **316**, 705 (2007).
- ⁵T. Killian, T. Pattard, T. Pohl, and J. Rost, “Ultracold neutral plasmas,” *Phys. Rep.* **449**, 77 (2007).
- ⁶S. Mayorov, A. Tkachev, and S. Yakovlenko, “Metastable supercooled plasma,” *Physics–Uspekhi* **37**, 279 (1994).
- ⁷A. Ignatov, V. Korotchenko, V. Makarov, A. Rukhadze, and A. Samokhin, “On the interpretation of computer simulation of classical Coulomb plasma,” *Physics–Uspekhi* **38**, 109 (1995).
- ⁸S. Mayorov, A. Tkachev, and S. Yakovlenko, “Comment on the article ‘On the interpretation of computer simulation of classical Coulomb plasma’ by A.M. Ignatov, A.I. Korotchenko, V.P. Makarov, A.A. Rukhadze, A.A. Samokhin,” *Physics–Uspekhi* **38**, 113 (1995).
- ⁹A. Bobrov, S. Bronin, B. Zelener, B. Zelener, E. Manykin, and D. Khikhlikha, “Collisional recombination coefficient in an ultracold plasma: Calculation by the molecular dynamics method,” *J. Exp. Theor. Phys.* **112**, 527 (2011).
- ¹⁰A. Lankin and G. Norman, “Collisional recombination in strongly coupled plasmas,” *J. Phys. A: Math. Theor.* **42**, 214042 (2009).
- ¹¹K. Niffenegger, K. Gilmore, and F. Robicheaux, “Early time properties of ultracold neutral plasmas,” *J. Phys. B* **44**, 145701 (2011).
- ¹²Y. Dumin, “Characteristic features of temperature evolution in ultracold plasmas,” *Plas. Phys. Rep.* **37**, 858 (2011).
- ¹³R. Fletcher, X. Zhang, and S. Rolston, “Using three-body recombination to extract electron temperatures of ultracold plasmas,” *Phys. Rev. Lett.* **99**, 145001 (2007).
- ¹⁴J. Ziman, *Principles of the Theory of Solids*, 2nd ed. (Cambridge Univ., Cambridge, UK, 1972).
- ¹⁵G. Demyanov and P. Levashov, “Systematic derivation of angular-averaged Ewald potential,” *J. Phys. A: Math. Theor.* **55**, 385202 (2022).
- ¹⁶Y. Dumin and A. Lukashenko, “Electron temperature relaxation in the clustered ultracold plasmas,” *Phys. Plasmas* **29**, 113506 (2022).
- ¹⁷Y. Dumin and A. Lukashenko, “Effects of disorder on electron heating in ultracold plasmas,” *Phys. Plasmas* **31**, 013502 (2024).
- ¹⁸W. Press, S. Teukolsky, W. Vetterling, and B. Flannery, *Numerical Recipes in Fortran 77: The Art of Scientific Computing*, 2nd ed., Vol. 1 (Cambridge Univ. Press, Cambridge, UK, 1992).
- ¹⁹A. Lankin and G. Norman, “Crossover from bound to free states in plasmas,” *J. Phys. A: Math. Theor.* **42**, 214032 (2009).
- ²⁰S. Tiwari, N. Shaffer, and S. Baalrud, “Thermodynamic state variables in quasiequilibrium ultracold neutral plasma,” *Phys. Rev. E* **95**, 043204 (2017).
- ²¹L. Landau and E. Lifshitz, *Mechanics*, 3rd ed. (Pergamon, Oxford, 1976).
- ²²T. Killian, M. Lim, S. Kulin, R. Dumke, S. Bergeson, and S. Rolston, “Formation of Rydberg atoms in an expanding ultracold neutral plasma,” *Phys. Rev. Lett.* **86**, 3759 (2001).